CrystEngComm

COMMUNICATION

View Article Online
View Journal | View Issue

Cite this: *CrystEngComm*, 2018, **20**, 2233

Received 27th March 2018,
Accepted 28th March 2018

DOI: 10.1039/c8ce00478a

rsc.li/crystengcomm

Molecular tectonics: control of crystalline sequences†

Cyril R. R. Adolf, Sylvie Ferlay * and Mir Wais Hosseini *

Following the molecular tectonics approach, the design and preparation of crystalline entities with controlled sequences were achieved by crystal welding processes based on isostructural and almost isometric coloured crystals. The strategy was based on stepwise 3D epitaxial growth.

Both for fundamental and applied sciences, the understanding and design of crystalline complex molecular systems with strict control of their short and long range orders both at the microscopic and macroscopic levels is of prime importance for the development of new solid state materials and devices. Hierarchical construction of crystalline species resulting from the interconnection of single crystals into networks of crystals leading to sequencing of crystalline zones may be a powerful tool for generating new crystalline task-specific materials. This may be achieved by the molecular tectonics approach[1] for which molecular crystals are considered as supramolecular entities[2,3] seen as periodic molecular networks[4] composed of interconnected complementary tectons[5] bearing within their framework specific geometric and recognition information. Beyond crystal engineering,[6] engineering multi-zone single crystals such as core–shell crystals[7–9] and welded crystals[10] remains a challenge. For the molecular tectonics approach, four different categories of molecular crystals may be defined (Fig. 1): a crystal, a molecular architecture possessing periodicity both in position and in composition (Fig. 1a); a crystalline solid solution, a periodic assembly in position but random in composition (Fig. 1b); a core–shell crystal composed of different interconnected crystalline zones, each periodic in position and in composition (Fig. 1c), this type of organization is obtained by stepwise hierarchical self-assembly processes, and finally a welded crystal, a multi-zone architecture composed of at least three domains periodic in position and in composition within each crystalline domain (Fig. 1d). This type of architecture may be obtained by a stepwise self-assembly strategy. It is worth noting that except for the molecular crystal, for a solid solution, the tectons need to be similar. For the other two categories, obtained by 3D epitaxial growth processes, the crystalline domains must be isostructural and almost isometric.

In this contribution, we report on the extensive use of crystal welding in solution and under mild conditions using 3D epitaxial growth for the generation of a variety of crystalline materials displaying controlled and imposed sequences.

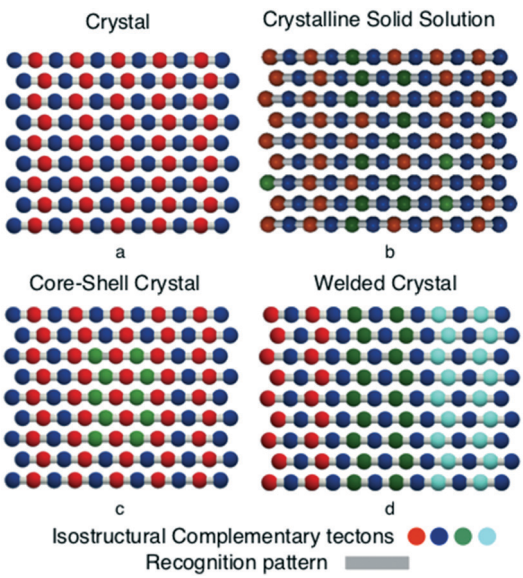

Fig. 1 Schematic representations (2D projections) of a portion of a) a crystal (periodic in position and in composition), b) a crystalline solid solution (periodic in position and random in composition), c) a core–shell crystal (periodic in position obtained by stepwise epitaxial growth) and d) a crystalline sequence (periodic in position displaying three crystalline zones). Red, blue and green spheres represent complementary tectons and the grey cylinder represents the recognition pattern connecting consecutive tectons.

Molecular Tectonics Laboratory, University of Strasbourg, CNRS, CMC UMR 7140, F-67000 Strasbourg, France. E-mail: ferlay@unistra.fr, hosseini@unisra.fr

† Electronic supplementary information (ESI) available: Synthesis of trimetallic 1D networks of crystals and their X-ray characterisation. See DOI: 10.1039/c8ce00478a

Among many possible attractive interactions that can be used for interconnecting consecutive tectons by self-assembly processes into periodic networks, directional H-bonding combined with charge–charge electrostatic interactions (charge-assisted H-bonding)[11] is particularly interesting.[1c,12]

Using such interactions, a variety of isostructural and almost isometric crystals have been generated by combining dicationic organic tectons and tetraanionic metallatectons as H-bond donors and acceptors, respectively.[12] Furthermore, they were used to form core–shell crystals by 3D epitaxial growth processes.[8] The same strategy was recently extended to the use of coordination bonds using metallatectons and metal cations.[9]

Combinations of the dicationic H-bond donor organic tecton $\mathbf{1}^{2+}$ with tetraanionic complexes $[ML_2]^{4-}$ (M = Mn, Fe, Co, Ni, Cu or Zn) as H-bond acceptors (Fig. 2) were shown to lead to the formation of robust isostructural (monoclinic, *C*2/*c*, *Z* = 4) and almost isometric crystals $\mathbf{1}_2$-ML_2 (see Table S1, ESI†).[10] The latter are based on the formation of 3D H-bonded networks between H-bond donor and acceptor tectons.

Interestingly, except for $\mathbf{1}_2$-ZnL_2 which is colourless, depending on the nature of the divalent cation (M = Mn, Fe, Co, Ni, Cu), coloured rod-type crystals are obtained (Fig. 3).[10] For the sake of clarity of description, $\mathbf{1}_2$-ML_2 (M = Mn, Fe, Co, Ni, Cu or Zn) crystals will be designated as **A**, **B** or **C** in the following sections.

In a preliminary investigation,[10] using a series of rod-type isostructural and almost isometric coloured crystals (Fig. 3), we have demonstrated that by 3D epitaxial growth, it is possible to generate, in solution and under mild conditions, core–shell crystals of type **B@A**. Furthermore, two crystals **A** aligned and oriented along the fastest growth axis *c* (Fig. 4a) may be fused in solution at room temperature into a welded single crystal **A**–**B**–**A** presenting the following sequence ***A*–*B*–*A*** (Fig. 4b). However, it must be noticed that since the welding process by 3D epitaxial growth takes place in solution, the growth phenomena operates at the two extremities of the welded crystal as well as at the other two directions of space *a* and *b* (Fig. 4b) leading thus to a welded core–shell crystal. Since the growth process is considerably faster along the *c* axis, by neglecting the growth along the *a* and *b* axes, the welded crystal may be seen as a crystal displaying a palindromic ***B*–*A*–*B*–*A*–*B*** sequence composed of five crystalline zones (Fig. 4c).

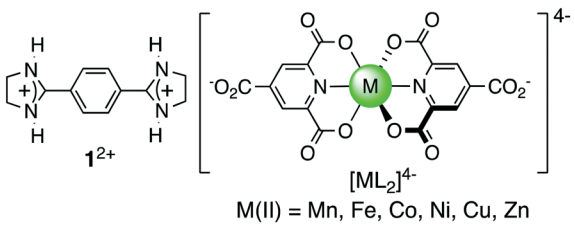

Fig. 2 Dicationic $\mathbf{1}^{2+}$ and tetraanionic $[ML_2]^{4-}$ (Mn, Fe, Co, Ni, Cu or Zn) tectons used for the formation of isostructural and almost isometric crystals.

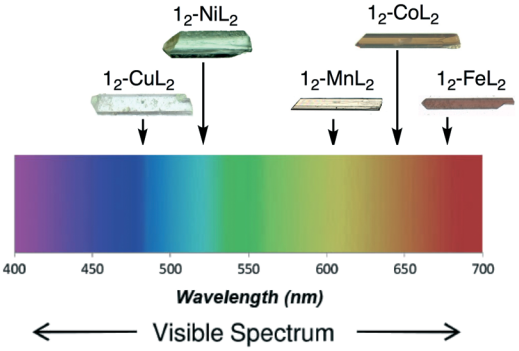

Fig. 3 Photographs of isostructural and almost isometric coloured rod-type crystals $\mathbf{1}_2$-ML_2 displaying absorption bands in the visible range.

The welding approach described above is rather versatile and may be further applied for the formation of strictly controlled sophisticated sequenced crystals. Indeed, instead of welding two identical crystals by a second crystalline phase (Fig. 4), the approach may be extended to the welding of two different crystals **A** and **B** (Fig. 5a) by a third crystalline domain **C** (Fig. 5b) leading to a non-symmetric sequence ***C*–*A*–*C*–*B*–*C*** presenting 5 different zones along the *c* axis (Fig. 5c).

It is worth noting that crystals $\mathbf{1}_2$-ML_2 (M = Mn, Fe, Co, Ni, Cu or Zn), possessing different colours, display a rod-type morphology with their extremities forming an angle with the fastest growth axis *c* (Fig. 3). We used these two observations to align the crystals along the *c* axis and to orient them. The orientation was further confirmed by face indexing. These two issues are crucial for optimal epitaxial growth.

In a Petri dish, two different crystals $\mathbf{1}_2$-FeL_2 and $\mathbf{1}_2$-CoL_2 were aligned and oriented along the *c* axis (Fig. 6a) and covered with a solution containing NiL_2^{4-} and $\mathbf{1}^{2+}$ cations, and the welding process was monitored using a macroscope (see the Experimental section, ESI†). The growth process led to the formation of the welded entity as a single crystal displaying the ***Ni*–*Fe*–*Ni*–*Co*–*Ni*** sequence (Fig. 6b). The single crystal nature of the latter was established by X-ray diffraction on the welded crystal. Furthermore, the cell parameters of different crystalline zones were determined by focussing the X-ray beam on the desired domains (see the Experimental characterisation section, ESI†).

The same procedure was applied to weld $\mathbf{1}_2$-FeL_2 and $\mathbf{1}_2$-MnL_2 crystals (Fig. 6c) by $\mathbf{1}_2$-NiL_2. The process afforded the unsymmetrical ***Ni*–*Fe*–*Ni*–*Mn*–*Ni*** sequence composed of 5

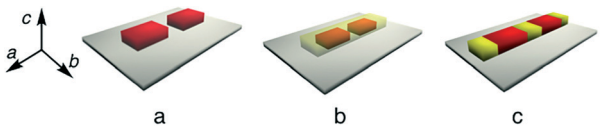

Fig. 4 Schematic representation of two aligned crystals **A** along the fastest growth axis *c* (a), welding of two crystals **A** by a crystalline phase **B** (b) and simplified representation of the welded crystal along the *c* axis leading to the palindromic ***B*–*A*–*B*–*A*–*B*** sequence (c). Crystals **A** and **B** differ in the nature of M in their $\mathbf{1}_2$-ML_2 units (see Fig. 1).

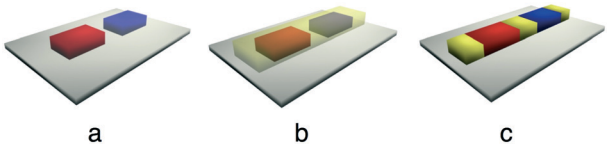

Fig. 5 Schematic representation of aligned crystals **A** and **B** along the fastest growth axis *c* (a), welding of crystals **A** and **B** by a crystalline phase **C** (b) and simplified representation of the welded crystal along the *c* axis leading to the unsymmetrical ***C–A–C–B–C*** sequence (c). Crystals **A**, **B** and **C** differ in the nature of M in their $\mathbf{1}_2$-ML_2 units (see Fig. 1).

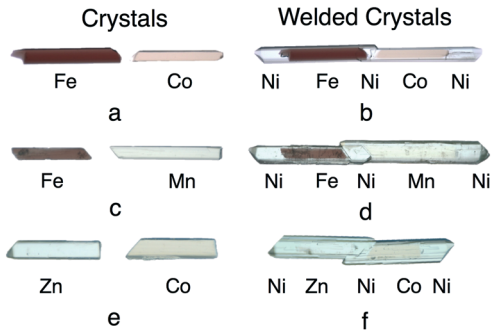

Fig. 6 Photographs of two aligned crystals along the *c* axis containing Fe and Co (a) and their welding by a crystalline phase containing Ni leading to the ***Ni–Fe–Ni–Co–Ni*** sequence (b), two crystals containing Fe and Mn (c) and their welding by a crystalline phase based on Ni leading to the ***Ni–Fe–Ni–Mn–Ni*** sequence (d) and two aligned crystals containing Zn and Co (e) and their welding by a crystalline phase based on Ni leading to the ***Ni–Zn–Ni–Co–Ni*** sequence (f).

crystalline interconnected zones (Fig. 6d). The generality of the strategy was further demonstrated by welding $\mathbf{1}_2$-ZnL_2 and $\mathbf{1}_2$-CoL_2 crystals (Fig. 6e) by $\mathbf{1}_2$-NiL_2 (Fig. 6f) displaying the ***Ni–Zn–Ni–Co–Ni*** sequence.

The stepwise strategy for the preparation of sequenced crystals by 3D epitaxial growth presented here is rather versatile and offers many design possibilities for the formation of crystalline mosaics composed of several zones. In particular, starting with a welded crystal presenting a ***B–A–B–A–B*** sequence (Fig. 7a), a core–shell crystal may be formed by epitaxial growth using a crystalline shell ***C*** (Fig. 7b). Again, by neglecting the growth along the *a* and *b* axes, the single crystal thus obtained may be described as displaying a ***C–B–A–B–A–B–C*** sequence along the *c* axis composed of seven crystalline domains (Fig. 7c).

Starting with a **Fe–Zn–Fe** welded crystal displaying a ***Zn–Fe–Zn–Fe–Zn*** sequence (Fig. 8a), the formation of the core–shell crystal **Ni@(Fe–Zn–Fe)** was achieved using a solution

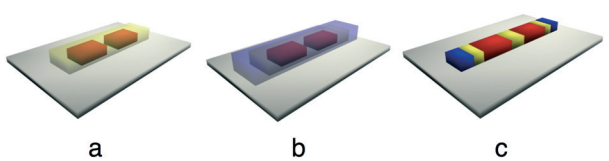

Fig. 7 Schematic representations of the welded crystal **A–B–A** (a) and the core–shell crystals **C@(A–B–A)** (b) leading to the ***C–B–A–B–A–B–C*** sequence (c) along the *c* axis.

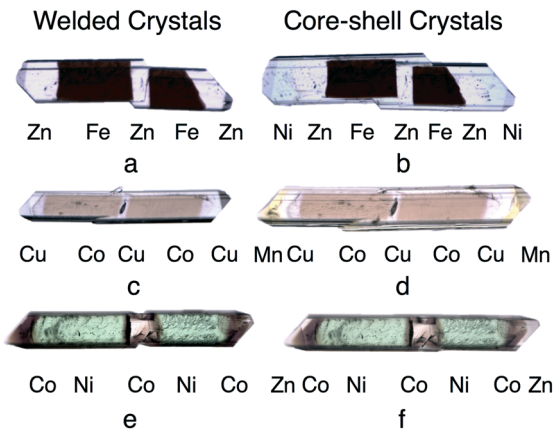

Fig. 8 Photographs of two Fe-based crystals welded by a Zn containing crystalline phase (a) and the core–shell crystal **Ni@(Zn–Fe–Zn–Fe–Zn)** with a ***Ni–Zn–Fe–Zn–Fe–Zn–Ni*** sequence (b), two Co-based crystals welded by a Cu containing phase (c) and the core–shell crystal **Mn@(Cu–Co–Cu–Co–Cu)** with a ***Mn–Cu–Co–Cu–Co–Cu–Mn*** sequence (d) and two Ni-based crystals welded by a Co containing crystalline phase (e) and the core–shell crystal **Zn@(Co–Ni–Co–Ni–Co)** with a ***Zn–Co–Ni–Co–Ni–Co–Zn*** sequence (f).

containing NiL_2^{4-} and $\mathbf{1}^{2+}$ (Fig. 8b). The latter is composed of a ***Ni–Zn–Fe–Zn–Fe–Zn–Ni*** sequence displaying seven crystalline zones. Starting with a **Co–Cu–Co** welded crystal displaying a ***Cu–Co–Cu–Co–Cu*** sequence (Fig. 8c), the same procedure using a solution containing MnL_2^{4-} and $\mathbf{1}^{2+}$ afforded the core–shell crystal **Mn@(Co–Cu–Co)** displaying a ***Mn–Cu–Co–Cu–Co–Cu–Mn*** sequence (Fig. 8d). Finally, starting with a **Ni–Co–Ni** welded crystal displaying a ***Co–Ni–Co–Ni–Co*** sequence (Fig. 8e), the same procedure using a solution containing ZnL_2^{4-} and $\mathbf{1}^{2+}$ produced the core–shell crystal **Zn@(Ni–Co–Ni)** composed of seven crystalline zones with a ***Zn–Co–Ni–Co–Ni–Co–Zn*** sequence (Fig. 8f).

In order to further extend the construction process, the formation of crystals composed of 9 zones was investigated. The strategy adopted may be based on the welding of two aligned and oriented core–shell crystals **B@A** (Fig. 9a) by a crystalline phase *C* leading to **(B@A)–C–(B@A)** welded crystals (Fig. 9b). Again, by neglecting the growth process along the *a* and *b* axes, the welded crystal displays a ***C–B–A–B–C–B–A–B–C*** sequence along the *c* axis (Fig. 9c).

Experimentally, the above mentioned strategy was demonstrated by welding two aligned and oriented core–shell crystals **(Cu@Co)** (Fig. 10a) using a solution containing NiL_2 and $\mathbf{1}^{2+}$ cations leading to a **(Cu@Co)–Ni–(Cu@Co)** single crystal (Fig. 10b). The latter displays along the *c* axis a symmetric

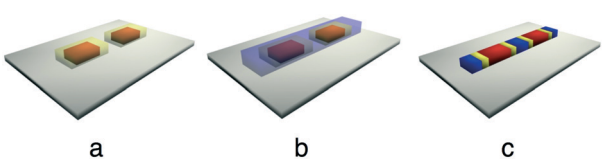

Fig. 9 Schematic representations of two aligned core–shell crystals ***B@A*** (a) and the welded crystal ***(B@A)–C–(B@A)*** by ***C*** (b) leading to a ***C–B–A–B–C–B–A–B–C*** sequence (c) along the *c* axis.

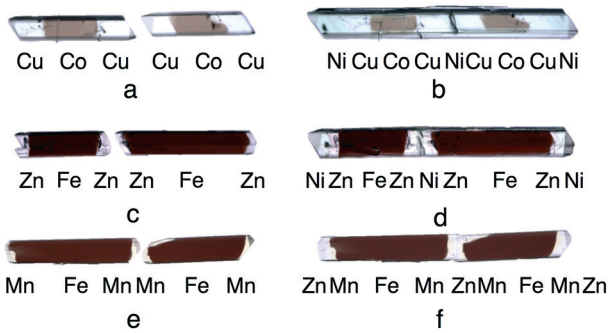

Fig. 10 Photographs of two core–shell crystals (**Cu@Co**) (a) welded by $\mathbf{1}_2$-NiL_2 (b), two core–shell crystals (**Zn@Fe**) (c) welded by $\mathbf{1}_2$-NiL_2 (d) and two core–shell crystals (**Mn@Fe**) (e) welded by $\mathbf{1}_2$-ZnL_2 (f) leading to crystals displaying palindromic sequences composed of nine crystalline zones.

Ni–Cu–Co–Cu–Ni–Cu–Co–Cu–Ni sequence. Starting with two aligned and oriented core–shell crystals (**Zn@Fe**) (Fig. 10c), the same procedure produced the welded crystal (**Zn@Fe**)–**Ni**–(**Zn@Fe**) displaying a ***Ni–Zn–Fe–Zn–Ni–Zn–Fe–Zn–Ni*** symmetric sequence composed of nine different crystalline zones (Fig. 10d). Finally, in order to verify the generality of the approach, two aligned and oriented core–shell crystals (**Mn@Fe**) (Fig. 10e) were welded using a solution containing ZnL_2 and $\mathbf{1}^{2+}$ cations leading to a (**Mn@Fe**)–**Zn**–(**Mn@Fe**) single crystal (Fig. 10f) displaying a ***Zn–Mn–Fe–Mn–Zn–Mn–Fe–Mn–Zn*** palindromic sequence along the *c* axis.

In conclusion, we have shown that, using a series of isostructural and almost isometric crystals differing by their colour, crystals with a controlled sequence along the fastest growth axis can be designed and generated using a welding strategy in solution under mild conditions. The crystalline entities obtained displaying 5, 7 or 9 crystalline zones may be of interest due to their optical properties owing to the differences in their refractive indices. The strategy presented here, although restricted to isostructural and almost isometric crystals, is rather versatile and may be applied to the design and preparation of a wide variety of molecular crystalline materials. Research along these lines is currently underway using other series of crystals.

Conflicts of interest

There are no conflicts to declare.

Acknowledgements

We thank the University of Strasbourg, the C.N.R.S., the International Centre for Frontier Research in Chemistry (icFRC), the Labex CSC (ANR-10-LABX-0026 CSC) within the Investissement d'Avenir program ANR-10-IDEX-0002-02, and the Ministère de l'Enseignement Supérieur et de la Recherche for financial support.

Notes and references

1 (*a*) M. Simard, D. Su and J. D. Wuest, *J. Am. Chem. Soc.*, 1991, **113**, 4696–4698; (*b*) S. Mann, *Nature*, 1993, **365**, 499–505; (*c*) M. W. Hosseini, *Acc. Chem. Res.*, 2005, **38**, 313–323.
2 J.-M. Lehn, *Supramolecular Chemistry, Concepts and Perspectives*, VCH, Weinheim, 1995.
3 J. D. Dunitz, *Pure Appl. Chem.*, 1991, **63**, 177–185.
4 M. W. Hosseini, *CrystEngComm*, 2004, **6**, 318–322.
5 (*a*) J. D. Wuest, *Chem. Commun.*, 2005, 5830–5837; (*b*) M. W. Hosseini, *Chem. Commun.*, 2005, 5825–5829.
6 (*a*) G. M. J. Schmidt, *Pure Appl. Chem.*, 1971, **27**, 647–678; (*b*) G. R. Desiraju, *Angew. Chem., Int. Ed. Engl.*, 1995, **34**, 2311–2327; (*c*) M. C. Etter, *Acc. Chem. Res.*, 1990, **23**, 120–126.
7 (*a*) J. C. MacDonald, P. C. Dorrestein, M. M. Pilley, M. M. Foote, J. L. Lundburg, R. W. Henning, A. J. Schultz and J. L. Manson, *J. Am. Chem. Soc.*, 2000, **122**, 11692–11702; (*b*) J. C. Noveron, M. S. Lah, R. E. Del Sesto, A. M. Arif, J. S. Miller and P. J. Stang, *J. Am. Chem. Soc.*, 2002, **124**, 6613–6625; (*c*) T.-J. M. Luo, J. C. MacDonald and G. T. R. Palmore, *Chem. Mater.*, 2004, **16**, 4916–4927; (*d*) K. Sada, K. Inoue, T. Tanaka, A. Epergyes, A. Tanaka, N. Tohnai, A. Matsumoto and M. Miyata, *Angew. Chem., Int. Ed.*, 2005, **44**, 7059–7062; (*e*) J. W. Steed, A. E. Goeta, J. Lipkowski, D. Swierczynski, V. Panteleon and S. Handa, *Chem. Commun.*, 2007, 813–815; (*f*) R. McNeil and P. Paukstelis, *J. Adv. Mater.*, 2017, **29**, 1701019; (*g*) C. M. Balogh, L. Veyre, G. Pilet, C. Charles, L. Viriot, C. Andraud, C. Thieuleux, F. Riobé and O. Maury, *Chem. – Eur. J.*, 2017, **23**, 1784–1788; (*h*) M. Pan, Y.-X. Zhu, K. Wu, L. Chen, Y.-J. Hou, S.-Y. Yin, H.-P. Wang, Y.-N. Fan and C.-Y. Su, *Angew. Chem., Int. Ed.*, 2017, **56**, 14582–14586.
8 (*a*) S. Ferlay and M. W. Hosseini, *Chem. Commun.*, 2004, 788–789; (*b*) P. Dechambenoit, S. Ferlay and M. W. Hosseini, *Cryst. Growth Des.*, 2005, **5**, 2310–2312; (*c*) P. Dechambenoit, S. Ferlay, N. Kyritsakas and M. W. Hosseini, *Chem. Commun.*, 2009, 1559–1561; (*d*) G. Marinescu, S. Ferlay, N. Kyritsakas and M. W. Hosseini, *Chem. Commun.*, 2013, 11209–11211.
9 F. Zhang, C. R. R. Adolf, N. Zigon, S. Ferlay, N. Kyritsakas and M. W. Hosseini, *Chem. Commun.*, 2017, **53**, 3587–3590.
10 C. R. R. Adolf, S. Ferlay, N. Kyritsakas and M. W. Hosseini, *J. Am. Chem. Soc.*, 2015, **137**, 15390–15393.
11 (*a*) K. T. Holman, A. M. Pivovar, J. A. Swift and M. D. Ward, *Acc. Chem. Res.*, 2001, **34**, 107–118; (*b*) M. W. Hosseini, *Coord. Chem. Rev.*, 2003, **240**, 157–166.
12 S. Ferlay and M. W. Hosseini, in *Functional Supramolecular Architectures for organic electronics and nanotechnology*, ed. P. Samori and F. Cacialli, Wiley-VCH, Weinheim, 2001, vol. 1, p. 195.

